World Journal of Gastrointestinal Pharmacology and Therapeutics

Submit a Manuscript: http://www.wjgnet.com/esps/
Help Desk: http://www.wjgnet.com/esps/helpdesk.aspx
DOI: 10.4292/wjgpt.v7.i3.416

World J Gastrointest Pharmacol Ther 2016 August 6; 7(3): 416-427
ISSN 2150-5349 (online)

ORIGINAL ARTICLE

Basic Study

Effects of aging on the architecture of the ileocecal junction in rats

Maria Cícera de Brito, Renato Paulo Chopard, Diego Pulzatto Cury, Ii Sei Watanabe, Cristina Eusébio Mendes, Patricia Castelucci

Maria Cícera de Brito, Diego Pulzatto Cury, Department of Surgery, Faculty of Veterinary Medicine and Animal Science, University of São Paulo, São Paulo 05508-900, Brazil

Renato Paulo Chopard, Diego Pulzatto Cury, Ii Sei Watanabe, Cristina Eusébio Mendes, Patricia Castelucci, Department of Anatomy/Biomedical Science Institute, University of São Paulo, São Paulo 05508-900, Brazil

Author contributions: de Brito MC performed all of the experiments and analyzed the results for this work; Chopard RP planned experiments; Cury DP and Watanabe IS helped and analyzed the transmission and scan electron microscopy studies; Mendes CE helped edit the manuscript and figures; Castelucci P planned the immunohistochemistry study, wrote and edit the manuscript.

Institutional review board statement: This study approved in the meeting of day 2/19/2014 and agree with Ethical principles in animal research adopted by ethic committee in the use of animals of the school of veterinary medicine and animal science of University of São Paulo.

Conflict-of-interest statement: No potential conflicts of interest relevant to this article were reported.

Data sharing statement: No additional data are available.

Correspondence to: Dr. Patricia Castelucci, PhD, Associate Professor, Department of Anatomy/Biomedical Science Institute, University of São Paulo, R. Dr. Lineu Prestes 2415, São Paulo 05508-900, Brazil. pcastel@usp.br

Telephone: +55-11-30918463
Fax: +55-11-30917366

Received: January 3, 2016
Peer-review started: January 4, 2016
First decision: February 26, 2016
Revised: March 15, 2016
Accepted: April 5, 2016
Article in press: April 6, 2016
Published online: August 6, 2016

Abstract

AIM: To evaluate the structural organization of the elastic and collagen fibers in the region of the ileocecal transition in 30 young and old male Wistar rats.

METHODS: Histology, immunohistochemistry (IHC), transmission electron microscopy and scanning electron microscopy were employed in this study. The results demonstrated that there was a demarcation of the ileocecal region between the ileum and the cecum in both groups.

RESULTS: The connective tissue fibers had different distribution patterns in the two groups. IHC revealed the presence of nitric oxide synthase, enteric neurons and smooth muscle fibers in the ileocecal junctions (ICJs) of both groups. Compared to the young group, the elderly group exhibited an increase in collagen type Ⅰ fibers, a decrease in collagen type Ⅲ fibers, a decreased linear density of oxytalan elastic fibers, and a greater linear density of elaunin and mature elastic fibers.

CONCLUSION: The results revealed changes in the patterns of distribution of collagen and elastic fibers that may lead to a possible decrease in ICJ functionality.

Key words: Ileocecal junction; Elastic fibers; Collagen fibers; Aging; Rats

Core tip: The ileocolonic sphincter controls the forward and backward flow by integrating its motility with that of the distal ileum and proximal the ileocolonic sphincter controls the forward and backward flow by integrating its motility with that of the distal ileum and proxima. The ileocecal junction (ICJ) includes the muscle bundles in the terminal ileum, the intrinsic nerve plexus. The ICJ includes the muscle bundles in the terminal ileum, the intrinsic nerve plexus. Given the importance of knowing how the ICJ changes with age, the objective of this study was to characterize the morphological changes in the ICJ in rats aged 21 d and 2 years, using optical microscopy and electronic scanning and transmission methodologies. Additionally, the neurochemical characterization of the inhibitory neurons of the myenteric plexus, which are immunoreactive to the enzyme nitric oxide synthase, and the staining of the neuronal population were employed to identify immunoreactivity to HuC/D.

de Brito MC, Chopard RP, Cury DP, Watanabe IS, Mendes CE, Castelucci P. Effects of aging on the architecture of the ileocecal junction in rats. *World J Gastrointest Pharmacol Ther* 2016; 7(3): 416-427 Available from: URL: http://www.wjgnet.com/2150-5349/full/v7/i3/416.htm DOI: http://dx.doi.org/10.4292/wjgpt.v7.i3.416

INTRODUCTION

The ileocecal junction (ICJ) has two aspects: A wedge-shaped cavity that progressively narrows the orifice to form the ileum and is bordered by an upper lip and lower lip, joined by front and posterior commissures; and an invagination of the small intestine to the large intestine[1-4]. Morphological differences between species can be related to the type of digestion, either partial or total, in the cecum[5-8]. The smooth muscle cells of the ICJ maintain a high tone[9]. The ileocolonic sphincter controls the forward and backward flow by integrating its motility with that of the distal ileum and proximal[9]. The ICJ includes the muscle bundles in the terminal ileum, the intrinsic nerve plexus, and the presence or absence of the interstitial cells of Cajal (ICC). Many ICC associated with the myenteric plexus are observed in both the ileal and cecal sides of the valve[10]. The neuronal density is lower in the cecum and ileal papilla compared to the terminal ileum. ICC exist within the myenteric plexus of the ICJ, and their density is similar to the adjacent bowel[4]. Histochemistry for acetylcholinesterase (AchE) and NADPH-diaphorase (NADPH-d) histochemistry and immunohistochemistry for protein gene product 9.5 (PGP 9.5) and C-kit in the ICJ revealed two distinct coaxial myenteric plexuses, together with superficial and deep submucosal plexuses. The C-kit immunostaining showed a continuous myenteric ICC network within the ICV[6].

Additionally, the ICJ is accompanied by a framework of collagen and elastic fibers[1-3,11]. The elastic fibers function to maintaining the elasticity of tissues throughout life[12]. Changes to the collagen arrangement and its three-dimensional (3D) distribution may be related to the dissimilar biomechanical proprieties in the terminal ileum[11]. Changes have been observed in the composition and architecture of the connective tissue with aging, resulting in the loss of elasticity and extensibility of different tissues[12,13].

The loss of ICJ function is clinically important. The loss of ICJ function may cause fecal reflux, with the risk of bacterial colonization in the terminal ileum[14]. Given the importance of knowing how the ICJ changes with age, the objective of this study was to characterize the morphological changes in the ICJ in rats aged 21 d and 2 years, using optical microscopy and electronic scanning and transmission methodologies. Additionally, the neurochemical characterization of the inhibitory neurons of the myenteric plexus, which are immunoreactive to the enzyme nitric oxide synthase (NOS), and the staining of the neuronal population were employed to identify immunoreactivity to HuC/D.

MATERIALS AND METHODS

We used 30 male Wistar rats (Rattus norvegicus) from the Central Animal Facility of the Institute of Biomedical Sciences, University of São Paulo in this study. The animals were housed in polypropylene cages that could hold up to three animals. The temperature was controlled at 21 ℃ ± 1 ℃, and the humidity was approximately 60%. The animals were maintained on alternating cycles of 12 h of light and 12 h of dark, with a balanced diet and water provided *ad libitum*. All the procedures were approved by the Ethics Committee on Animal Experiments of the Faculty of Veterinary Medicine and Animal Science of the University of São Paulo. The animals were divided into two groups: (1) a young group, 21 d old (n = 15); and (2) an older group, 24 mo old (n = 15). Each group was analyzed using microscopy (n = 7), immunohistochemistry (IHC; n = 2), transmission electron microscopy (TEM; n = 2) and scanning electron microscopy (SEM; n = 4).

Histology methods

For light microscopy, the animals were euthanized with an overdose of xylazine (40 mg/kg) and ketamine (120 mg/kg) and then the ICJ was removed. The samples were fixed in 10% paraformaldehyde fixative for 24 h at room temperature before undergoing routine histological processing. Cuts were made in the longitudinal direction with a thickness of 5 μm using a Reichert Jung ultramicrotome. Samples were stained using hematoxylin and eosin (HE). Elastic fibers were revealed by staining with iron hematoxylin (Verhoeff), resulting in blue and

Table 1 Characteristics of the primary and secondary antibodies used in this study

Antigen	Host	Dilution	Source
Nitric oxide synthage	Sheep	1:1000	Chemicon
HuC/D	Mouse	1:100	Molecular probes
Anti-sheep IgG 488	Donkey	1:100	Molecular probes
Anti-mouse IgG 594	Donkey	1:200	Molecular probes

black tones[15-17]. Staining with resorcin-fuchsin (Weigert), with and without oxone, showed mature elastic fibers as pink, and elaunin and oxytalan were stained in shades of purple and black[16,17].

Picrosirius staining under polarized light allowed the observation of collagen birefringence, allowing the classification of the type or age of the collagen according to the color and light intensity of the refringence. Polarized light of picrosirius-stained samples evidenced yellow and red fibers (type Ⅰ collagen) and green fibers (type Ⅲ collagen). The stained slides were observed and digitized with a NIKON Eclipse E600 microscope and NIS-Elements AR software for documentation and further qualitative and quantitative analysis.

IHC fluorescence method

For IHC, the animals were euthanized with an overdose of xylazine (40 mg/kg) and ketamine (120 mg/kg). After collection, the samples were washed by immersion in phosphate-buffered saline solution (PBS; 1.15 mol/L NaCl and 0.01 mol/L sodium phosphate buffer, pH = 7.2), and then they were washed with PBS. After this procedure, the samples were sectioned by mesenteric margins and were subsequently fixed in wooden rafts with the mucosa facing down with the aid of pins. Subsequently, the sections were immersed in 4% paraformaldehyde fixative in 0.1 mol/L sodium phosphate buffer, pH 7.3 at 4 ℃ for 24 h. On the following day, the samples were removed from the fixative and washed in PBS three times with intervals of 10 min each. Then, some of the samples were stored in PBS containing sodium azide (0.1%) at 4 ℃ for preservation, and the others were transferred to PBS + 30% sucrose for 24 h at 4 ℃. The next day, an exchange of substances in 50:50 PBS + 30% sucrose + Optimum Cutting Temperature Tissue Tek, Elkhart (OCT) was performed, and the samples were stored overnight. After this period, the switch was made at 100%. The samples were then stored at -80 ℃ to maintain their conservation. After the completion of all the procedures mentioned above, the samples were fixed on metal bases (stubs) in 10 μm slices, and cuts were made with an 1850 Leica cryostat at -25 ℃. The sections were mounted on slides, which were stored at room temperature for 1 h and then immersed in 10% normal horse serum solution (NHS) and 1.5% Triton (Sigma) in PBS for 45 min at room temperature. Then, the samples were incubated with primary antibody (Table 1) for 48 h.

After 24 h, the samples were again subjected to washes with PBS (three times for 10 min each) and were further incubated with a secondary antibody (Table 1). The tissues were immersed in 2.6-diamino-2-phenylindole dihydrochloride (DAPI) for five minutes to stain the nuclei of all the cells. Subsequently, the tissues were washed in PBS (3 times for 5 min each). Then, the slides were covered with a glycerol coverslip buffered in 0.5 mol/L calcium carbonate buffer (pH 8.6). Observations were performed with a Nikon 80i fluorescence microscope using the Nis Elements program. Sample preparations were also analyzed with a confocal scanning microscope (Olympus Fluorview FV10SW Laser).

TEM method

After pre-anesthesia, the animals were perfused with a modified Karnovsky fixative solution containing 2.5% glutaraldehyde and 2% paraformaldehyde in 0.1 mol/L sodium phosphate buffer at pH 7.4[18]. After perfusion, samples were collected from the ICJ. The samples were post-fixed in 2.5% glutaraldehyde for 2 h at 4 ℃. They were then washed in sodium phosphate buffer and post-fixed in 1% osmium tetroxide for 2 h at 4 ℃. The samples were washed with brine, and then were immersed in 0.5% uranyl acetate overnight. On the following day, the samples were dehydrated in a series of increasing alcohol concentrations (from 2% to 70%) before baths in absolute alcohol and propylene oxide for 15 min each. The samples were then embedded in a mixture of Spurr® resin. The samples were placed in shallow molds of silicone, which were then placed in an oven at 60 ℃ for 48 h for polymerization of the resin. The blocks were then subjected to trimming, and thin sections from 0.5 μm to 1 μm were obtained with an ultra-microtome. The sections were then collected on glass slides, stained with toluidine blue and washed with 1% distilled water for observation by light microscopy for the delimitation of areas. Ultrathin sections approximately 70 nm thick were made and collected in 200 mesh copper screens. The sections were contrasted with 4% uranyl acetate solution for 10 min and were then washed with distilled water[18] and 4% lead citrate for 10 min[18]. All the cuts were made with an ultra-microtome (Leica Ultracut, Germany) in the multiuser laboratory of the Department of Biomedical Sciences Institute of Anatomy, University of São Paulo. The sections were analyzed by TEM (Fei Morgagni 265 and Jeol 1010 brand microscopes set to 80 kV).

SEM method

For SEM, the animals were anesthetized intraperitoneally with ketamine (60 mg/kg) and xylazine (20 mg/kg) and then were perfused with a fixative solution of modified Karnovsky containing 2.5% glutaraldehyde, 2% paraformaldehyde, and a 0.1 mol/L solution of sodium phosphate buffer at pH = 7.4[18]; approximately 60 mL of solution was injected through the left ventricle of the heart. After perfusion, samples from the ICJ were then removed and immersed in fixative for 48 h at 4 ℃. Then, the tissues were sectioned at the mesenteric margin.

Some of the samples were selected for SEM, and some were subjected to treatment with a 5% aqueous solution of sodium hydroxide (NaOH)[19,20], which was changed daily for 4 d; the samples were then washed in distilled water for 2 d at 4 ℃. After this step, all the samples (sectioned and macerated) were post-fixed in aqueous 1% osmium tetroxide for 2 h at 4 ℃ and dehydrated in a series of increasing alcohol concentrations and dried in a critical point apparatus (Balzers CPD-020) using liquid CO_2. After drying, the samples were mounted on aluminum metal bases and subjected to a metal cover with gold ions in the "sputtering" unit (Union Balzers SCD 040).

Quantitative analysis

Collagen fibers: The study of the collagen fiber system was performed by capturing random fields using the Imaging Software NIS program - Elements AR 3.1 for the observation of collagen types Ⅰ and Ⅲ. Six fields of each slide were captured with a × 20 lens. From these images, collagen fiber type Ⅰ (red) and type Ⅲ (green) densities were quantified with a software tool that recognizes color variations in an image using the color channels of red, green and blue (RGB). This software allows the identification of one color at a time, yielding the average color intensity of the given area and the area of each field equivalent to 274252.78 pixels[21].

Elastic fibers: The histomorphometrical examination was performed using linear density (Ld) estimation of the elastic system. The estimated elastic fiber length was derived from the formula L = 2Q × EV, where L = length of the elastic fiber structure per unit volume, Q = number of cross-sectioned elastic fibers in the plane of the section and EV = unit volume. The fiber length per unit volume is directly proportional to the number of fiber intersections within the unit section area[21-23]. The samples were analyzed with a 100X lens, immersion oil, and eye Kf 10 × 18 compensation, with 117 points integration, showing 13 parallel lines vertically and 9 horizontally. The total area was 117000 μm^2. The distance (L) between the points in this system was 10 μm according to the procedure reported[24]. Histological sections of the ICJ were observed and documented under a microscope (Nikon Eclipse E600/NIS - Elements).

Statistical analysis

A statistical analysis was performed by comparing the linear density of the collagen and elastic fibers of the young and elderly groups. The data were analyzed statistically using Student's *t*-test with a significance level of $P < 0.05$.

RESULTS

Histological analyses

The HE staining showed that smooth muscle cells were distributed in the mucosa and submucosa of the intestine in both groups, and both regions showed an arrangement in three different muscle layers: Two circular layers and one longitudinal muscle layer, with their cores in the central portion of the cells (Figure 1A-D). Spaces between smooth muscle cells were observed in the young group (Figure 1A, B); however, in the older group (Figure 1C, D), connective tissue fiber condensation between the smooth muscle cells was observed. The transition region had different cell characteristics. The ileum protruded into the cecum, while thickening occurred in the circular muscle layer. The cecum of both groups comprised a glandular epithelium without villi (Figure 1A-D).

Picrosirius staining under non-polarized light (Figure 1E and G) showed the general appearance of the ICJ. Picrosirius staining under polarized light showed the architecture of the Type Ⅰ and Type Ⅲ collagen fibers of the ICJ in both groups. These fibers were arranged around the smooth muscle cells and originated from both sides of the cecal ileum to form the transition surface. In addition, evaluating the structure of the connective framework revealed a clear predominance of type Ⅰ collagen fibers, which was characteristic of mature tissue in the elderly group (Figure 1H), that were shorter, thicker and more numerous. Note that the type Ⅰ collagen fibers in the young group (Figure 1F) were more elongated and thin and were less prevalent compared to the elderly group. Type Ⅲ collagen fibers were more numerous in the young group (Figure 1F) and were thinner compared to the older group (Figure 1H).

Elastic fibers: Weigert staining with previous oxidation showed oxytalan fibers (Figure 2A and B). In the young group (Figure 2A), these fibers were arranged in parallel, were thinner compared to the elderly group (Figure 2B), and were thicker and curved. Weigert staining (Figure 2C) also showed elaunin fibers. These fibers were arranged in parallel and were straight and slender in the young group (Figure 2C), which was different from the observations in the elderly group (Figure 2D) in which these fibers were more curved and thick. With Verhoeff staining (Figure 2E and F), it was possible to identify mature elastic fibers in both groups. These showed more slender and straight fibers in the young group (Figure 2E). However, in the elderly group (Figure 2F) these fibers were thicker, shorter and more crooked.

IHC: Immunoreactive neurons and fibers were identified by HuC/D (Figure 3A and D) and NOS (Figure 3B, E) in the young and elderly groups. The nuclei of the smooth muscle cells were identified by DAPI staining (Figure 3C and D). Figure 3C and F shows the triple labeling of immunoreactive neurons with NOS, HuC/D and DAPI. There was a homogeneous distribution of cytoplasmic immunoreactivity for HuC/D and NOS in the myenteric neurons of both groups.

TEM: In the young group (21-d-old), the observation of the mucosa of the ileocecal transition region revealed the presence of smooth muscle cells sectioned transversely

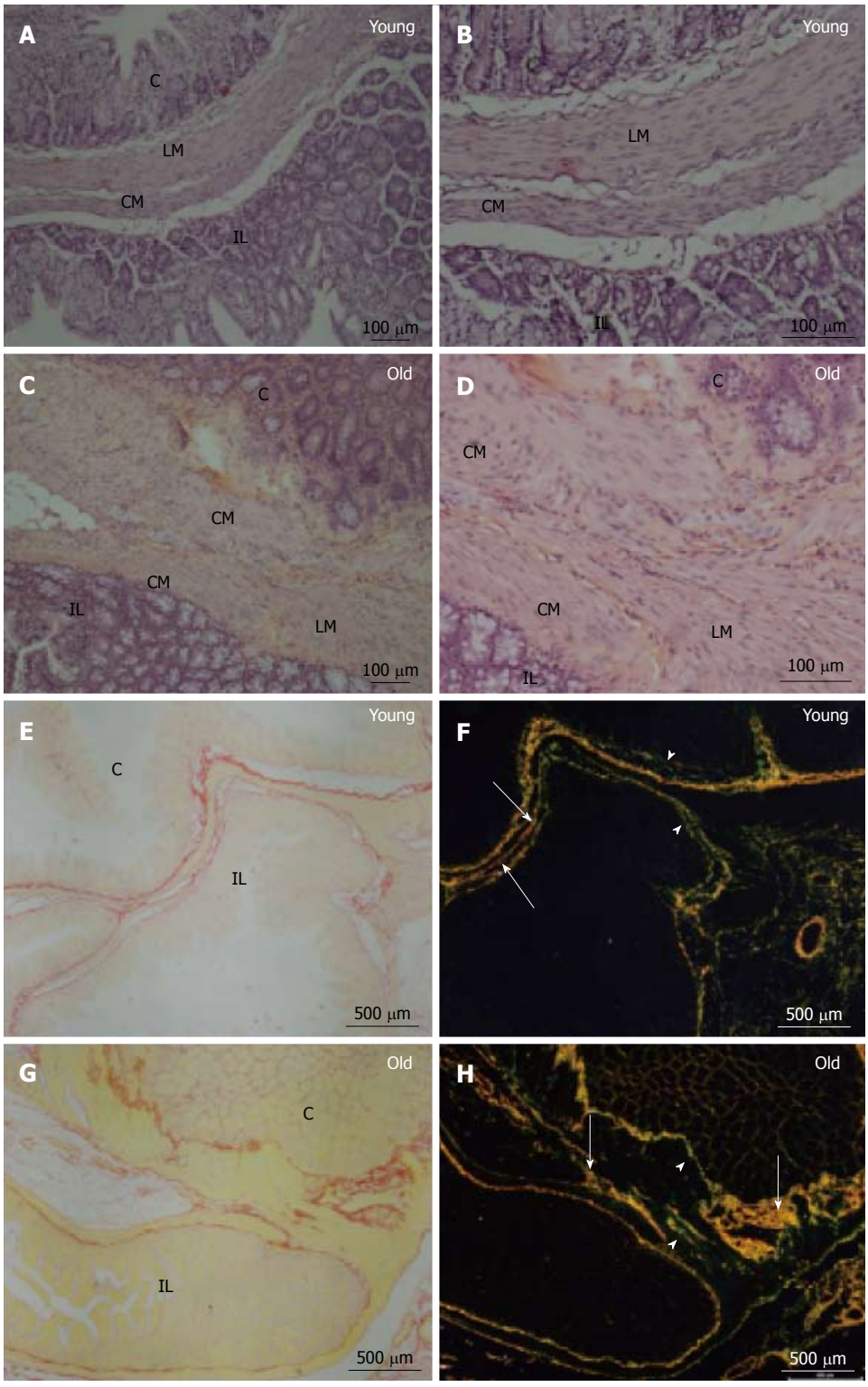

Figure 1 Histological sections of the ileocecal junctions in the young group and the elderly group. Hematoxylin-eosin staining (A-D) was performed to examine the ileum (IL), cecum (C), circular muscle layer (CM) and longitudinal muscle layer (ML). Picrosirius staining under non-polarized light (E and G) showed the transition region between the ileum (IL) and cecum (C). Picrosirius staining under polarized light (F and H) showed type I collagen fibers (yellow, orange and red) (arrows) and type III collagen fibers (green) (arrowhead).

(Figure 4A). The smooth muscle cells were surrounded by bundles of collagen fibers (Figure 4A and B). Between muscle cells, we observed numerous unmyelinated fibers (Figure 4B). The nerve fibers contained neurofilaments and mitochondria (Figure 4B). In the elderly group (24-mo-old), longitudinal sections were observed (Figure 4C). Between muscle fibers in the elderly group, there was a larger amount of collagen fibers forming the

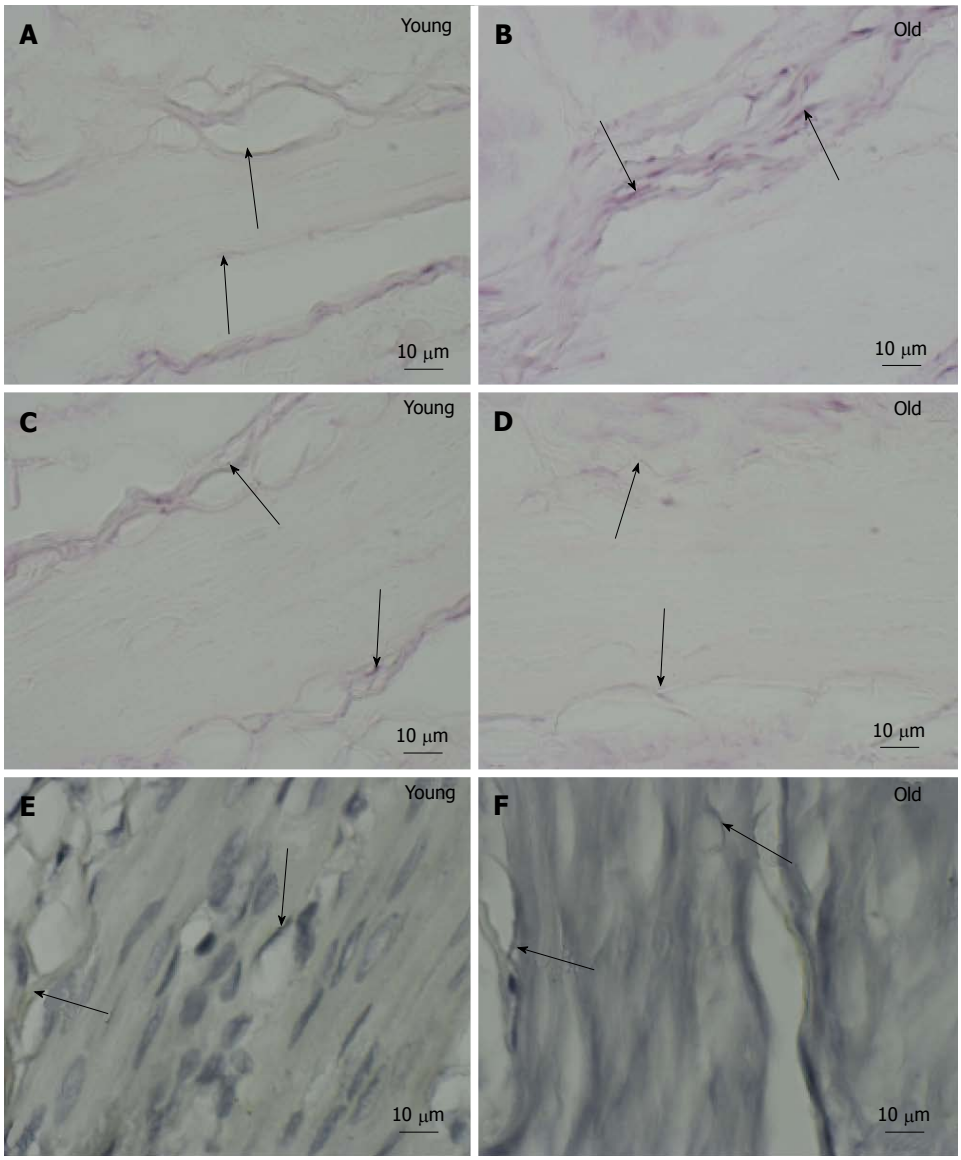

Figure 2 Histological sections of ileocecal junctions in the young group (A, C, E) and the elderly group (B, D, F) stained with Weigert with oxone (A, B), Weigert (C, D) and Verhoeff (E, F).

endomysium of the cells (Figure 4C). There were many unmyelinated nerve fibers of different diameters (Figure 4D).

SEM

SEM of ileocecal transition segment samples from the young and elderly groups revealed the transition region, with mucosal projections of the ileal and cecal regions (Figure 5). In the young group, the mucosal surface of the transition between the ileum and cecum showed a perfectly demarcated area where numerous elongated buds had formed on the microvilli in the ileum region (Figure 5A and B). After treatment with sodium hydroxide solution, the cell layers were completely removed and the ileocecal transition region was clearly identified, revealing numerous foramens in the cecum. There were foramens and laminar projections of collagen fibers in the ileum (Figure 5C and D); however, the cecal region had only foramens without collagen (Figure 5D).

In the elderly group, the line delimiting the two regions was visible as a surface containing a groove (Figure 5E). A characteristic, normal-looking mucosa forming the microvilli was observed (Figure 5F). After treatment with a sodium hydroxide solution, the epithelial-tissue interface regions of the ileum and cecum showed that the ileum region had numerous laminar projections of collagen fibers interspersed with an essentially circular foramen (Figure 5G). In the region of the cecum, numerous circular and elongated foramens in a three-dimensional arrangement were observed (Figure 5H).

Quantitative analysis

An analysis of light intensity after picrosirius staining under polarized light showed that the value for the average linear type Ⅰ collagen fibers in the young group

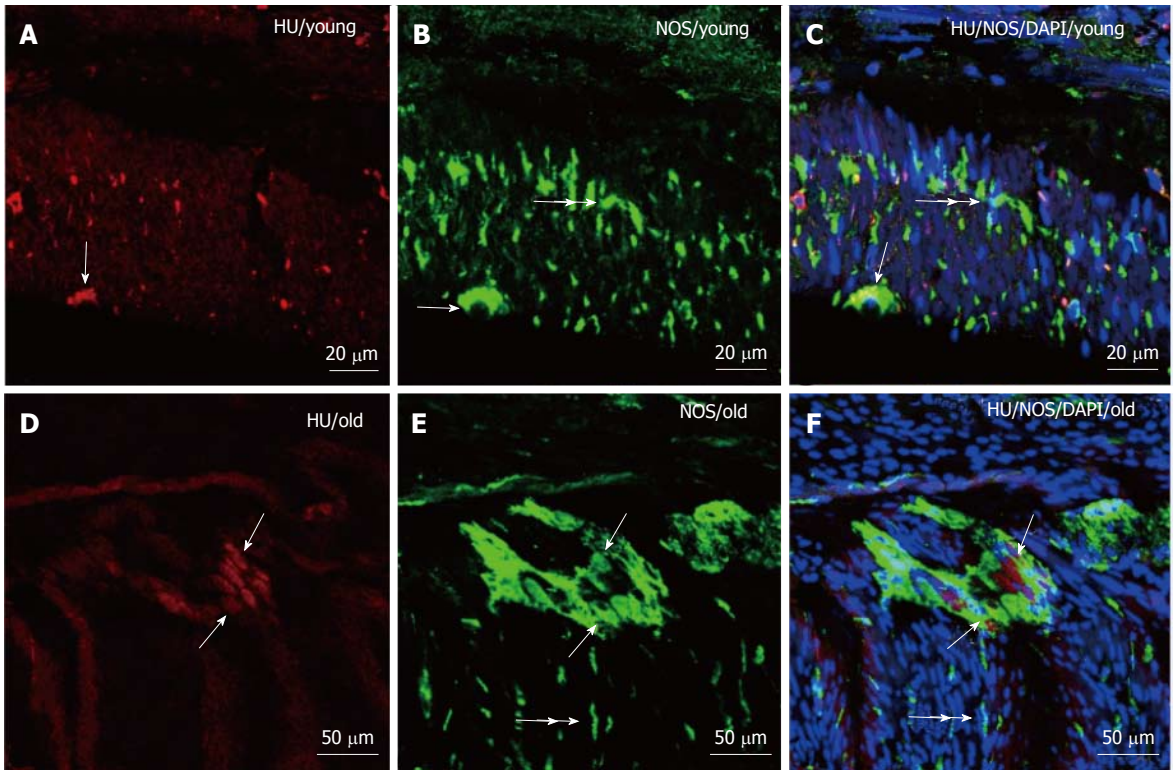

Figure 3 Immunohistochemistry mistry final. HuC/D staining in immunoreactive neurons (A, D), NOS staining in immunoreactive neurons and nerve fibers (B, E), and DAPI staining of the nuclei of immunoreactive cells (C, F) of the ileocecal junction in young rats (A-C) and elderly rats. The co-localization of HuC/D, NOS and DAPI (C, F). The arrows indicate immunoreactive neurons stained for HuC/D (A, D), NOS (B, E), and triple colocalization with HuC/D, NOS and DAPI (C, F). The double arrows indicate immunoreactive fibers stained for NOS (B, E). The double arrows show muscle fiber nuclei stained with DAPI (C, F). NOS: Nitric oxide synthage; DAPI: 4',6-diamidino-2-phenylindole.

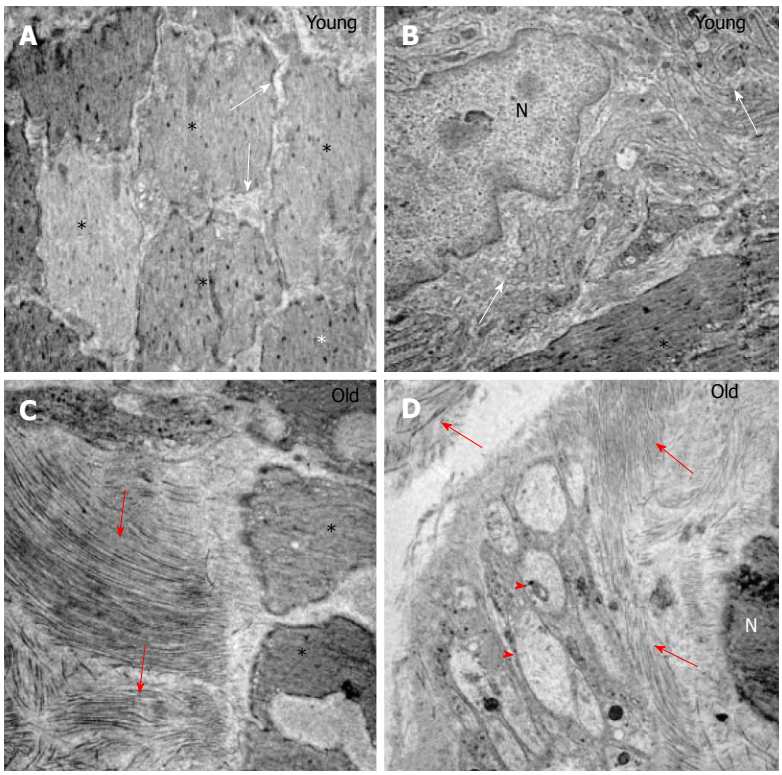

Figure 4 Transmission electron microscopy. A: A cross-section of the muscle layer showing the muscle fibers (*) and connective tissue (arrow) of the young group. Magnification: × 6000; B: A longitudinal section of the muscle layer showing muscle fibers (*), nuclei (N) and a set of unmyelinated fibers (arrows) of the young group Magnification: × 20000; C: A longitudinal section of the muscular layer showing collagen fibers arranged in different directions (arrows) and muscle fibers of the elderly group. Magnification: × 10000; D: Nucleus (N) and collagen fibers arranged in different directions (arrows) and synaptic vesicles (arrowhead) of the elderly group. Magnification: × 10000.

was 10842.7 ± 212.6 pixels. The elderly group had a mean linear value of 16465.4 ± 184.4 pixels, a significant increase of 51.9% ($P < 0.001$) compared to that in the young group (Figure 6A). The average linear value of type Ⅲ collagen fibers in the young group was 21706.4 ± 47.9 pixels. The elderly group showed a mean linear

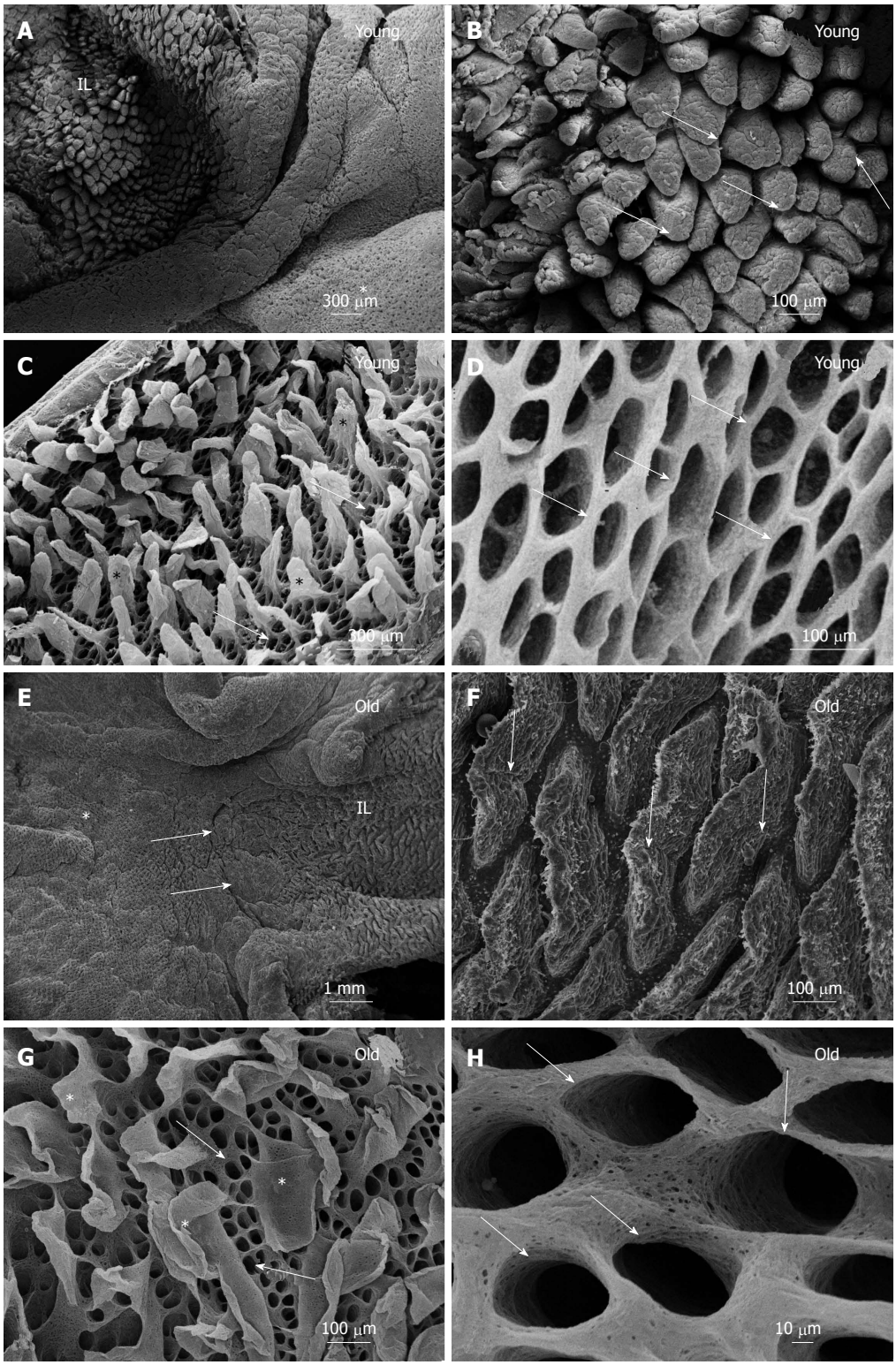

Figure 5 Normal mucosa of the rat ileocecal transition point of the young and elderly groups. A: Normal mucosa of the rat ileocecal transition point of the young showing the ileum (IL) and cecum (*); B: Villi with a normal appearance (arrows); C: Sample treated with NaOH solution. Image showing the connective tissue with different forms of blades (*) and numerous foramens (arrows) in a network of collagen fibers; D: Image showing the interphase cell surface tissue of the cecum, including the foramen; E: Ileum (IL), cecum (*) and ileocecal junction (arrows) of the elderly group; F: The highest increase in ileal villi (arrows); G: Sample treated with NaOH solution. Ileum tissue-shaped blade (*) and numerous foramens as a network of collagen fibrils (arrows). Image showing the foramen cecum surface (arrows).

value of 20876.9 ± 60.4 pixels, a significant decrease of 3.8% ($P < 0.001$) compared to the young group (Figure 6A).

The results for elaunin, which were obtained from samples stained with resorcin-fuchsin (Weigert), showed that the average linear density was 0.00692 ± 0.00015/

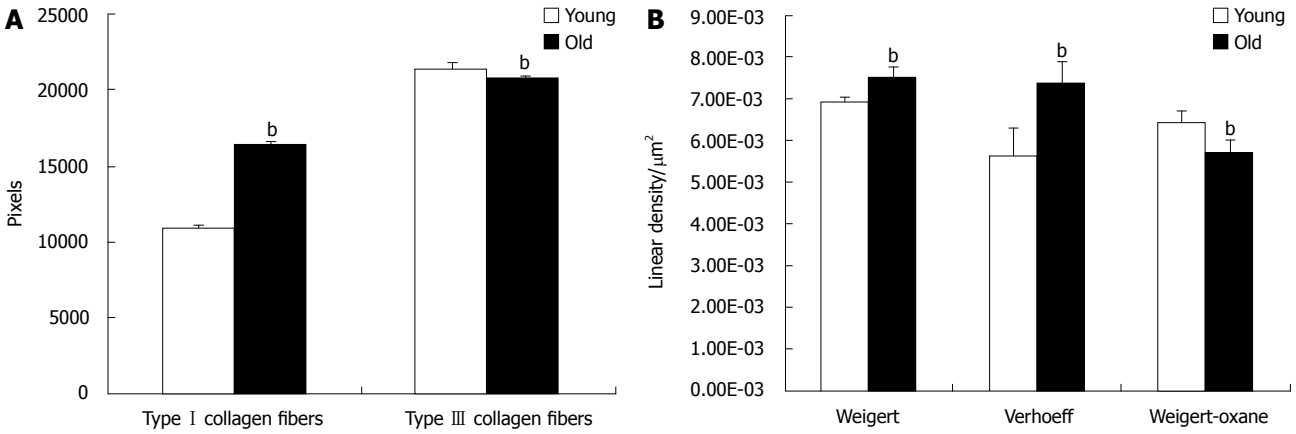

Figure 6 Quantitative analysis. Data related to the means ± SD of the mean linear (pixels) of type Ⅰ and type Ⅲ collagen (A) and data indicating the linear density (LD) expressed as the mean ± SD of oxytalan elastic fibers (Weigert) (μm^2), elaunin fibers (Verhoeff) (μm^2), and mature elastic fibers (Weigert-Oxane) (μm^2) (B) of the young and old groups. $^bP < 0.001$.

μm^2 in the young group and 0.0075 ± 0.00023/μm^2 in the elderly group, a significant increase of 8.7% in the elderly group compared to the young group ($P < 0.001$; Figure 6B). Regarding the mature elastic fibers that underwent Verhoeff staining, the mean linear density was 0.00564 ± 0.00067/μm^2 in the young group and 0.0074 ± 0.00049/μm^2 in the elderly group, a significant increase of 31.2% ($P < 0.001$) in the elderly group compared to the young group (Figure 6B). After oxytalan, resorcin, and fuchsin staining (Weigert) and after oxidation with a 1% aqueous solution of oxone, the linear density of the fibers in the young group was 0.0064 ± 0.0067 μm^2, and that in the elderly group was 0.00575 ± 0.00027/μm^2. There was a significant decrease of 10.3% in the elderly group compared to that in the young group ($P = 0.001$; Figure 6B).

DISCUSSION

This study examined and compared the ICJ structures of young and aged rats. Histological analysis revealed that connective tissue fibers and smooth muscle cells were present in the ICJs of both groups. The ileum protruded into the cecum, as reported[4], who used human ICJ samples and reported that the muscle layers of the ileum and large intestine extended into the ileal papilla. In this study, we observed a thickening and narrowing of the smooth muscle layer in both groups, as reported[1-4,10].

Histologically, the elderly group exhibited a condensation of the connective tissue between smooth muscle cells in the transition; however, the young group displayed noticeable gaps between the smooth muscle fibers, which likely indicate limited development of collagen fibers. Similar results were described in colons of humans at different ages[25]; their data indicated that the connective tissue was more slender in the young group but had a larger amount of collagen and elastic fibers around the myenteric plexus in older individuals. Our results demonstrated that smooth muscle cells of the ICJ were distributed with three distinct muscle layers, *i.e.,* two circular muscle layers and a longitudinal layer, as also observed[10]. In the transition region, there was a thickening of the circular muscle layer, as previously observed[4].

The present data revealed the presence of NOS in the ICJ. Furness[26] (2006) emphasized that NOS catalyzes the formation of the NO that is present in the myenteric plexus and neuronal processes in the gut, which acts to relax the muscle fiber function of the gastrointestinal musculature. Previous studies have shown the presence of NOS in the enteric ganglia and muscle fibers under various conditions, such as malnutrition and renutrition[27,28], ischemia and reperfusion[29-31] and obesity[32,33]. The enteric neurons of the ICJ stain positive for NOS, PGP 9.5, and c-kit[3,4,6,8]. Additionally, neuronal nitric oxide synthase (nNOS) is present in the myenteric, the submucosal ganglia and the IJC muscle layers in horse[8]. In our study, we noticed the presence of NOS in the muscle layers and neurons in the ICJs of both the young and elderly groups, but we did not observe a difference in the intensity of the stain for HuC/D or NOS between groups. Major losses of enteric neurons occur during aging; these losses have been described in both the myenteric and submucous plexus ganglia of all regions of the gut in several mammalian species[24,34]. Regarding significant changes in the number of myenteric neurons during aging in several species, including humans[35,36], previous studies have suggested the possible involvement of the regulation of gastrointestinal functions. Moreover, Hoyle and Saffrey[37] (2012) stressed that the thickening of the circular muscle layer is due to increased contractility during aging.

In our ultrastructural analysis, both groups had smooth muscle cells with elongated nuclei between these collagen fibers, forming an endomysium of smooth muscle cells. In the group of older animals, the collagen fibers were thicker. The mitochondria in both groups had different shapes and sizes. It should be noted that, in this study, the mitochondria were not quantified, but they appeared to be present in greater quantity in the elderly group. In agreement with observations obtained in this study,

the authors reported that in the submucosal plexus of the small intestine of rats at different ages, mitochondria were present in greater numbers in the elderly group and had a degenerative aspect[38]. In the process of aging, changes in cell morphology occur that include the presence of pleomorphic mitochondria[39].

The SEM results in both groups revealed a clear demarcation of the transition region, which was bounded by a line of flat connective tissue between the ileum and the cecum. In the ileum, numerous elongated buds were present, constituting microvilli. The villus morphology seemed to depend on age, exhibiting a sheet form, which has been predominantly reported in children. However, this form is present in adults as fingerlike projections[40]. Collagen fibers were present on both sides of the cecal ileum, forming the transition surface. In the cecal portion, low laminar-form microvilli were observed, as were numerous foramens of regular collagen fibers with interconnected formats.

Our results showed that the type Ⅰ collagen fibers in the elderly group were more bulky and appeared thicker; they were classified as mature collagen. These fibers were resistant to traction and tension, giving strength to the tissue. In contrast, in the young group, we noticed a predominance of type Ⅲ collagen fibers, which were thinner and were characterized as immature collagen, which produces flexibility in the tissue. In accordance with the results observed[38], the elderly group exhibited a replacement of type Ⅲ collagen with type Ⅰ collagen around the submucosal plexus of the jejunum and ileum compared to the young group. This finding suggests that changes in the distribution of collagen fibers could damage the function of the submucosal ganglia. Also, authors reported an increase in the number of collagen fibers in the aorta of aged mice[41]. In addition, authors showed that aging favored an increase in the diameter of collagen fibrils[42], in agreement with our findings. Additionally, both collagen and elastic system fibers were more numerous in the enteric ganglia from the old subjects[25]. Changes in the distribution pattern of collagen fibers in the ICJ can lead to intestinal disorders, such as decreased motility and changes in the retrograde return of feces, which consequently leads to the inflammation of the ileal mucosa. Therefore, the replacement of the collagen in the ICJ is not beneficial to the operating mechanism of the intestinal segment.

During aging, changes occur in the architecture of the collagen fibers, compromising the biomechanical and biochemical properties of tissues due to an accumulation of advanced glycation end-products (AGEs)[43]. The authors also suggested that aging structurally changes the collagen monomer, which greatly affects both the fibrillogenesis process and the architecture of the collagen fibers.

Additionally, our results reveal that elastic fibers were identified by staining with Weigert oxone, Weigert and Verhoeff, indicating that three types of the elastic system fibers were present along the smooth muscles of the ICJ. The linear density analysis revealed that oxytalan fibers were in greater quantity in the young group and were diminished in the elderly group. Similar results in the gastroduodenal junctions of young and old animals were reported[21]. In the present work, the linear density of elaunin fibers and elastic fibers was increased in the elderly group compared to the young group, and oxytalan fibers was decreased in the elderly group compared to the young group. Similar results were described by[44,45], who found that during aging, there was a decrease in oxytalan fibers and an increase mature elaunin and elastic fibers. Furthermore, elastin was thicker and more fragmented in older people, and there was a greater deposition of calcium in the amorphous material. In a study of aging cerebral meninges, reported decreases and increases in the oxytalan fiber contents of mature elaunin and elastic fibers, respectively[46]. In studies on the vas deferens reinforced these findings, stating that there was an increase in elastin during aging[47]. Moreover, study of the interspinous ligament during aging found the disappearance of oxytalan fibers[48], which is in agreement with our results. In addition to our study, authors suggested that aging is accompanied by a significant and progressive reduction in oxytalan fibers and significant increases in mature elaunin and elastic fibers in the interfoveolar ligament[44].

Elaunin fibers play an intermediary role between oxytalan fibers and mature elastic fibers, providing functional adaptation in different tissues. Based on the results, the function of the ICJ appears to change with aging, which is associated with changes in the patterns of distribution of collagen and elastic fibers, resulting in increased tensile strength and firmness, but decreased elasticity. With the decrease in the ICJ, oxytalan fibers can lose complacency, becoming less flexible, looser and less able to retreat. Moreover, increased amounts of mature elaunin and elastic fibers are present. We suggest that, with the gradual reduction of the elastic components and replacement of the collagen types in the fibers, ICJ function loss occurs due to the loss of elasticity and the resultant decreased distensibility.

Finally, we highlight the importance of the results of our morphoquantitative analysis of changes in the connective tissue of the ICJ in young and elderly groups, which revealed changes in the patterns of distribution of collagen and elastic fibers that may lead to a possible decrease in ICJ functionality, which may favor the occurrence of pathological processes. These results do not elucidate all the aspects of ICJ function; additional studies should be conducted in the future.

ACKNOWLEDGMENTS

We thank Rosana Prisco for performing the statistical analysis and Sonia Regina Yokomizo Marta Maria da Silva Righetti, Sebastião Aparecido Boleta and Kelly Patricia Nery Borges for technical assistance.

COMMENTS

Background

The ileocecal junction (ICJ) has two aspects: A wedge-shaped cavity that progressively narrows the orifice to form the ileum and is bordered by an upper lip and lower lip, joined by front and posterior commissures; and an invagination of the small intestine to the large intestine.

Research frontiers

The neurochemical characterization of the inhibitory neurons of the myenteric plexus, which are immunoreactive to the enzyme nitric oxide synthase, and the staining of the neuronal population were employed to identify immunoreactivity to HuC/D.

Innovations and breakthroughs

The authors highlight the importance of the results of our morphoquantitative analysis of changes in the connective tissue of the ICJ in young and elderly groups, which revealed changes in the patterns of distribution of collagen and elastic fibers that may lead to a possible decrease in ICJ functionality, which may favor the occurrence of pathological processes.

Peer-review

The aim of the paper was to analyze the structural organization of the elastic and collagen fibers in the region of the ileocecal transition in 30 young and old male Wistar rats by using different updating techniques. The study is original, interesting and well conducted.

REFERENCES

1 **Ferraz de Carvalho CA**, Rodrigues de Souza R, Henrique A, Henrique A, Nogueira de Lima MA. Functional anatomy of the tela submucosa of the valva ileocecalis in the adult man. *Anat Anz* 1987; **164**: 63-76 [PMID: 3662029]
2 **Shafik AA**, Shafik A, Asaad S, Wahdan M. A study of an anatomic-physiological cecocolonic sphincter in humans. *Clin Anat* 2010; **23**: 851-861 [PMID: 20641065 DOI: 10.1002/ca.21026]
3 **Shafik AA**, Ahmed IA, Shafik A, Wahdan M, Asaad S, El Neizamy E. Ileocecal junction: anatomic, histologic, radiologic and endoscopic studies with special reference to its antireflux mechanism. *Surg Radiol Anat* 2011; **33**: 249-256 [PMID: 21184079 DOI: 10.1007/s00276-010-0762-x]
4 **Pollard MF**, Thompson-Fawcett MW, Stringer MD. The human ileocaecal junction: anatomical evidence of a sphincter. *Surg Radiol Anat* 2012; **34**: 21-29 [PMID: 21863224 DOI: 10.1007/s00276-011-0865-z]
5 **Kumar D**, Phillips SF. The contribution of external ligamentous attachments to function of the ileocecal junction. *Dis Colon Rectum* 1987; **30**: 410-416 [PMID: 3595357 DOI: 10.1007/BF02556486]
6 **Cserni T**, Paran S, Kanyari Z, O'Donnell AM, Kutasy B, Nemeth N, Puri P. New insights into the neuromuscular anatomy of the ileocecal valve. *Anat Rec* (Hoboken) 2009; **292**: 254-261 [PMID: 19089903 DOI: 10.1002/ar.20839]
7 **Vidotti AP**, Didio LJA, Prado MIM. Caracterização morfológica da região de Transição entre o intestino delgado e o grosso no javali. *Brazilian J Veterin Res Animal Sci* 2007; **44**: 151-158
8 **Russo D**, Bombardi C, Grandis A, Furness JB, Spadari A, Bernardini C, Chiocchetti R. Sympathetic innervation of the ileocecal junction in horses. *J Comp Neurol* 2010; **518**: 4046-4066 [PMID: 20737599 DOI: 10.1002/cne.22443]
9 **Malbert CH**. The ileocolonic sphincter. *Neurogastroenterol Motil* 2005; **17** Suppl 1: 41-49 [PMID: 15836454 DOI: 10.1111/j.1365-2982.2005.00657.x]
10 **Miyamoto-Kikuta S**, Ezaki T, Komuro T. Distribution and morphological characteristics of the interstitial cells of Cajal in the ileocaecal junction of the guinea-pig. *Cell Tissue Res* 2009; **338**: 29-35 [PMID: 19823824 DOI: 10.1007/s00441-009-0854-2]
11 **Prado IM**, Di Dio LJ, Miranda-Neto MH, Molinari SL, Macchiarelli G. Three-dimensional distribution of the collagen fibers in the submucosa of the swine terminal ileum. *Ital J Anat Embryol* 2005; **110**: 77-86 [PMID: 16101024]
12 **Kielty CM**, Sherratt MJ, Shuttleworth CA. Elastic fibres. *J Cell Sci* 2002; **115**: 2817-2828 [PMID: 12082143]
13 **Cotta-Pereira G**, Rodrigo FG, David-Ferreira JF. The elastic system fibers. *Adv Exp Med Biol* 1977; **79**: 19-30 [PMID: 68662 DOI: 10.1007/978-1-4684-9093-0_3]
14 **Quigley EM**, Thompson JS. Effects of artificial ileocolonic sphincter on motility in intestinal remnant following subtotal small intestinal resection in the dog. *Dig Dis Sci* 1994; **39**: 1222-1229 [PMID: 8200254 DOI: 10.1007/BF02093787]
15 **Fullmer HM**, Lillie J. The oxytalan fiber: a previously undescribed connective tissue fiber. *Journal of Histochemistry and Cytochemistry* 1958; **6**: 425-430 [PMID: 13598878]
16 **Bittencourt-Sampaio S**, Cotta-Pereira G, Guerra-Rodrigo F. Oxytalan, elaunin and elastic fibers in the human skin. *J Invest Dermatol* 1971; **66**: 143-148 [PMID: 1249442]
17 **Cotta-Pereira G**, Rodrigo FG, David-Ferreira JF. The use of tannic acid-glutaraldehyde in the study of elastic and elastic-related fibers. *Stain Technol* 1976; **51**: 7-11 [PMID: 59416]
18 **Watanabe I**, Yamada E. The fine structure of lamellated nerve endings found in the rat gingiva. *Arch Histol Jpn* 1983; **46**: 173-182 [PMID: 6882151 DOI: 10.1679/aohc.46.173]
19 **Ohtani O**. Three-dimensional organization of the connective tissue fibers of the human pancreas: a scanning electron microscopic study of NaOH treated-tissues. *Arch Histol Jpn* 1987; **50**: 557-566 [PMID: 3326543 DOI: 10.1679/aohc.50.557]
20 **Kronka MC**, Watanabe I, Cavenaghi Pereira da Silva M, König Júnior B. Corrosion casts of young rabbit palatine mucosa angioarchitecture. *Ann Anat* 2000; **182**: 529-531 [PMID: 11125803 DOI: 10.1016/S0940-9602(00)80097-7]
21 **Brito MC**, Cury DP, Barbosa ACS, Silva P.M, Chopard RP. Morphological and morphometric study of collagen and elastic fibers of the gastroduodenal junction of adult and old Wistar rats. *J Morphol Sci* 2013; **30**: 281-288
22 **Chopard RP**, Lucas GA, Gerhard R, Lourenço MG. A histomorphological study in age related changes in the elastic fiber system of the basilar artery. *Ital J Anat Embryol* 1998; **103**: 157-175 [PMID: 9882958]
23 **Chopard RP**, Gerhard R. Histomorphometrical study of the elastic fiber system in the anterior cerebral artery of man. *Arq Neuropsiquiatr* 2000; **58**: 1040-1046 [PMID: 11105071 DOI: 10.1590/S0004-282X2000000600011]
24 **Niewoehner DE**, Kleinerman J. Morphometric study of elastic fibers in normal and emphysematous human lungs. *Am Rev Respir Dis* 1977; **115**: 15-21 [PMID: 835883]
25 **Gomes OA**, de Souza RR, Liberti EA. A preliminary investigation of the effects of aging on the nerve cell number in the myenteric ganglia of the human colon. *Gerontology* 1997; **43**: 210-217 [PMID: 9222749 DOI: 10.1159/000213852]
26 **Furness JB**. The enteric nervous system. Malden: Blackwell Publishing Inc., 2006
27 **Misawa R**, Girotti PA, Mizuno MS, Liberti EA, Furness JB, Castelucci P. Effects of protein deprivation and re-feeding on P2X2 receptors in enteric neurons. *World J Gastroenterol* 2010; **16**: 3651-3663 [PMID: 20677337 DOI: 10.3748/wjg.v16.i29.3651]
28 **Girotti PA**, Misawa R, Palombit K, Mendes CE, Bittencourt JC, Castelucci P. Differential effects of undernourishment on the differentiation and maturation of rat enteric neurons. *Cell Tissue Res* 2013; **353**: 367-380 [PMID: 23644765 DOI: 10.1007/s00441-013-1620-z]
29 **Paulino AS**, Palombit K, Cavriani G, Tavares-de-Lima W, Mizuno MS, Marosti AR, da Silva MV, Girotti PA, Liberti EA, Castelucci P. Effects of ischemia and reperfusion on P2X2 receptor expressing neurons of the rat ileum enteric nervous system. *Dig Dis Sci* 2011; **56**: 2262-2275 [PMID: 21409380 DOI: 10.1007/s10620-011-1588-z]
30 **Palombit K**, Mendes CE, Tavares-de-Lima W, Silveira MP, Castelucci P. Effects of ischemia and reperfusion on subpopulations of rat enteric neurons expressing the P2X7 receptor. *Dig Dis Sci* 2013; **58**: 3429-3439 [PMID: 23990036 DOI: 10.1007/s10620-013-2847-y]

31 **Marosti AR**, da Silva MV, Palombit K, Mendes CE, Tavares-de-Lima W, Castelucci P. Differential effects of intestinal ischemia and reperfusion in rat enteric neurons and glial cells expressing P2X2 receptors. *Histol Histopathol* 2015; **30**: 489-501 [PMID: 25400134]

32 **Mizuno MS**, Crisma AR, Borelli P, Castelucci P. Expression of the P2X receptor in different classes of ileum myenteric neurons in the female obese ob/ob mouse. *World J Gastroenterol* 2012; **18**: 4693-4703 [PMID: 23002338 DOI: 10.3748/wjg.v18.i34.4693]

33 **Mizuno MS**, Crisma AR, Borelli P, Schäfer BT, Silveira MP, Castelucci P. Distribution of the P2X2 receptor and chemical coding in ileal enteric neurons of obese male mice (ob/ob). *World J Gastroenterol* 2014; **20**: 13911-13919 [PMID: 25320527 DOI: 10.3748/wjg.v20.i38.13911]

34 **Phillips RJ**, Powley TL. Innervation of the gastrointestinal tract: patterns of aging. *Auton Neurosci* 2007; **136**: 1-19 [PMID: 17537681 DOI: 10.1016/j.autneu.2007.04.005]

35 **Santer RM**, Baker DM. Enteric neuron numbers and sizes in Auerbach's plexus in the small and large intestine of adult and aged rats. *J Auton Nerv Syst* 1988; **25**: 59-67 [PMID: 3225382 DOI: 10.1016/0165-1838(88)90008-2]

36 **Saffrey MJ**. Cellular changes in the enteric nervous system during ageing. *Dev Biol* 2013; **382**: 344-355 [PMID: 23537898 DOI: 10.1016/j.ydbio.2013.03.015]

37 **Hoyle CH**, Saffrey MJ. Effects of aging on cholinergic neuromuscular transmission in isolated small intestine of ad libitum fed and calorically-restricted rats. *Neurogastroenterol Motil* 2012; **24**: 586-592 [PMID: 22435850 DOI: 10.1111/j.1365-2982.2012.01913.x]

38 **Zanesco MC**, Souza RR. Morphoquantitative study of the submucous plexus (of Meissner) of the jejunum-ileum of young and old guinea pigs. *Arq Neuropsiquiatr* 2011; **69**: 85-90 [PMID: 21359429 DOI: 10.1590/S0004-282X2011000100017]

39 **Silva WJM,** Ferrari CKB. Mitochondrial metabolism, free radicals and aging. *Revista Brasileira de Geriatria e Gerontologia* 2011; **14**: 441-451 [DOI: 10.1590/S1809-98232011000300005]

40 **Kim SB**, Barone B, Secreto HRC, Silva MRR, Egami MJ, Secreto RA, Juliano Y. Morfologia e morfometria da parede do íleo terminal de camundongos expostos ao raio x. *Acta cirurgica Brasileira* 1994; **9**: 174-182

41 **Cheng JK**, Stoilov I, Mecham RP, Wagenseil JE. A fiber-based constitutive model predicts changes in amount and organization of matrix proteins with development and disease in the mouse aorta. *Biomech Model Mechanobiol* 2013; **12**: 497-510 [PMID: 22790326 DOI: 10.1007/s10237-012-0420-9]

42 **Floridi A**, Ippolito E, Postacchini F. Age-related changes in the metabolism of tendon cells. *Connect Tissue Res* 1981; **9**: 95-97 [PMID: 6458452 DOI: 10.3109/03008208109160246]

43 **Wilson SL**, Guilbert M, Sulé-Suso J, Torbet J, Jeannesson P, Sockalingum GD, Yang Y. A microscopic and macroscopic study of aging collagen on its molecular structure, mechanical properties, and cellular response. *FASEB J* 2014; **28**: 14-25 [PMID: 24025727 DOI: 10.1096/fj.13-227579]

44 **Quintas ML**, Rodrigues CJ, Yoo JH, Rodrigues Junior AJ. Age related changes in the elastic fiber system of the interfoveolar ligament. *Rev Hosp Clin Fac Med Sao Paulo* 2000; **55**: 83-86 [PMID: 10983010 DOI: 10.1590/S0041-87812000000300003]

45 **Rodrigues Junior AJ**, Rodrigues CJ, da Cunha AC, Jin Y. Quantitative analysis of collagen and elastic fibers in the transversalis fascia in direct and indirect inguinal hernia. *Rev Hosp Clin Fac Med Sao Paulo* 2002; **57**: 265-270 [PMID: 12612758]

46 **Pereira KF**, Lima VM, Conegero CI, Chopard RP. Histomorfometria das meninges encefálicas de ratos Wistar em diferentes faixas etárias. *Pesquisa Veterinária Brasileira* 2010; **30**: 996-1002 [DOI: 10.1590/S0100-736X2010001100015]

47 **Paniagua R**, Regadera J, Nistal M, Santamaría L. Elastic fibres of the human ductus deferens. *J Anat* 1983; **137** (Pt 3): 467-476 [PMID: 6654739]

48 **Barros EM**, Rodrigues CJ, Rodrigues NR, Oliveira RP, Barros TE, Rodrigues AJ. Aging of the elastic and collagen fibers in the human cervical interspinous ligaments. *Spine J* 2002; **2**: 57-62 [PMID: 14588289 DOI: 10.1016/S1529-9430(01)00167-X]

P- Reviewer: de Talamoni NGT, Pescatori M **S- Editor**: Qi Y
L- Editor: A **E- Editor**: Lu YJ

Published by **Baishideng Publishing Group Inc**
8226 Regency Drive, Pleasanton, CA 94588, USA
Telephone: +1-925-223-8242
Fax: +1-925-223-8243
E-mail: bpgoffice@wjgnet.com
Help Desk: http://www.wjgnet.com/esps/helpdesk.aspx
http://www.wjgnet.com